ELSEVIER

Coordination Chemistry Reviews
190–192 (1999) 975–1002

COORDINATION CHEMISTRY REVIEWS

www.elsevier.com/locate/ccr

Electron deficient bonding of benzoheterocycles to triosmium clusters: synthesis and applications to organic chemistry

Md. Joynal Abedin [a], Brian Bergman [a], Richard Holmquist [a], Ryan Smith [a], Edward Rosenberg [a,*], Joana Ciurash [b], Kenneth Hardcastle [b], Jay Roe [b], Vanessa Vazquez [b], Candace Roe [b], Shariff Kabir [c], Biplob Roy [c], Shahana Alam [c], Kazi A. Azam [c]

[a] *Department of Chemistry, The University of Montana, Missoula, MT 59812-1006, USA*
[b] *Department of Chemistry, California State University, Northridge, CA 91330, USA*
[c] *Department of Chemistry, Jahangirnagar University, Savar, Dhaka, Bangladesh*

Received in revised form 16 February 1999

Contents

* Corresponding author. Tel.: +1-406-243-2592; fax: +1-406-243-4227.
E-mai address: rosen@selway.umt.edu (E. Rosenberg)

PII: S0010-8545(99)00154-X

Abstract

A new synthetic methodology for the addition of carbon based nucleophiles to the carbocyclic ring of quinolines has been developed which is based on the electron deficient bonding of the C(8) carbon and the protective coordination of the nitrogen atom to the metal core in the complexes $[Os_3(CO)_9(\mu_3\text{-}\eta^2\text{-}C_9H_5(R)N)(\mu\text{-}H)]$ (R can be a wide range of substituents in the 3-, 4-, 5- and 6-positions of the quinoline ring). These complexes react with a wide range of carbanions (R′Li, R′ = Me, ^{n}Bu, ^{t}Bu, Bz, Ph, $CH{=}CH_2$, $C_2(CH_2)_3CH_3$, CH_2CN, $(CH_3)_2CCN$, $-CHS(CH_2)_2S-$; $CH_2CO_2^t$Bu, R′MgBr, R′ = CH_3, $CH_2CH{=}CH_2$) to give the nucleophilic addition products $[Os_3(CO)_9(\mu_3\text{-}\eta^3\text{-}C_9H_7(5\text{-}R')N)(\mu\text{-}H)]$ (**2a**–**2l**), after quenching with trifluoracetic acid, in isolated yields of 43–86%. Substitution at the 3- or 4-position is well tolerated giving the expected nucleophilic addition products $[Os_3(CO)_9(\mu_3\text{-}\eta^3\text{-}C_9H_6(3 \text{ or } 4\text{-}R)(5\text{-}R')N)(\mu\text{-}H)$. The 6-substituted derivatives give > 95% of the *cis*-diastereomer, $[(Os_3(CO)_9(\mu_3\text{-}\eta^3\text{-}C_9H_6(5\text{-}R')(6\text{-}R)N)(\mu\text{-}H)]$. The stereochemistry is preserved even in the case of less bulky carbanions (R′ = CH_3). In the case of the 6-Cl derivative, a second product is obtained on reaction with the isobutyryl carbanion, $[Os_3(CO)_9(\mu_3\text{-}\eta^2\text{-}C_9H_5(6\text{-}Cl)(5\text{-}C(CH_3)_2CN)N)(\mu\text{-}H)_2]$ (**4**) which is the result of protonation at the metal core and rearrangement of the carbocyclic ring. The *trans*-diastereomer of the addition products obtained from the 6-substituted derivatives can be synthesized by reaction of the unsubstituted complex with R′Li followed by quenching with $(CH_3O)_2SO_2$. Acetic anhydride can also be used as the quenching electrophile for the intermediate anions generated from R′Li $[(trans\text{-}Os_3(CO)_9(\mu_3\text{-}\eta^3\text{-}C_9H_6\text{-}(6\text{-}CH_3CO)(5\text{-}CH_3)N)(\mu\text{-}H)]$ (**5**). Nucleophilic addition occurs across the 3,4-bond in the cases where the 5-position is occupied by a substituent. The nucleophilic addition products can be rearomatized by reaction with DBU/DDQ or by reaction of the intermediate anion with trityl cation or DDQ. The resulting rearomatized complexes can be cleanly cleaved from the cluster by reflux in acetonitrile under a CO atmosphere yielding the functionalized quinoline and $Os_3(CO)_{12}$ as the only two products. An overview of this previously reported work along with additional examples of this novel chemistry is given here as well as an extention of the synthesis of the electron deficient triosmium clusters to a wide range of heterocycles structurally related to quinoline. These complexes include those containing the heterocycles: phenanthridine (**7**), 5,6-benzoquinoline (**8**), 2-CH_3-benzimidazole (**9**), 2-methyl benzotriazole (**10**), 2-methyl-benzoxazole (**11**), 2-R-benzothiazole (R = H, **12**; CH_3, **13**) and quinoxaline (**14**). The solid state structures of **7**–**10**, **12**, and **14** are reported.

Keywords: Osmium; Clusters; Nucleophilic Addition; Quinolines; Benzoheterocycles; Carbanions

1. Introduction

The transition metal activated nucleophilic addition and substitution reactions of π-bound arenes have proven to be an extremely useful addition to the organic chemist's arsenal for functionalizing arenes, cyclizations and asymmetric syntheses [1–3]. Recently, this methodology has been extended to include bicyclic arenes, heterocycles [4] and indoles [3,5]. Notably missing from this group of substrates for

nucleophilic activation by transition metals is the quinoline family. This is primarily because quinoline prefers η^1-N coordination over η^6-coordination to the carbocyclic ring, in sharp contrast to indoles, due to their greater basicity [6]. There are thus few π-η^6-arene complexes of quinoline and nucleophilic addition and substitution has been studied only for the η^1-N transition metal complexes [7]. We recently reported the synthesis of a family of σ-μ_3-η^2 complexes of quinoline which undergo regioselective nucleophilic addition of hydride and a wide range of carbanions at the 5-position (Eqs. 1 and 2) [8–11].

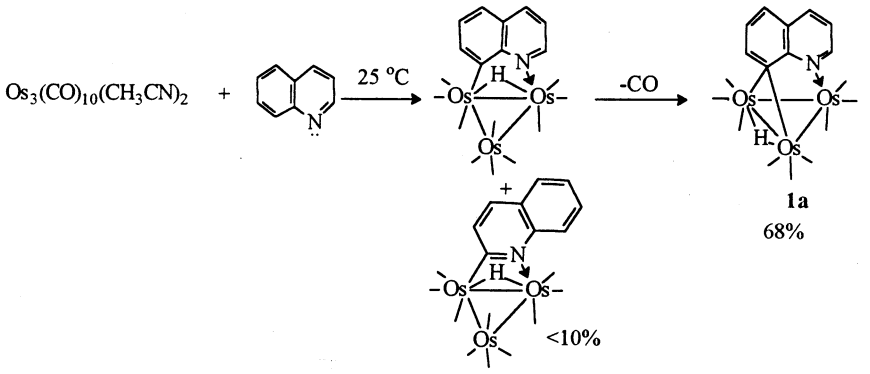

(1)

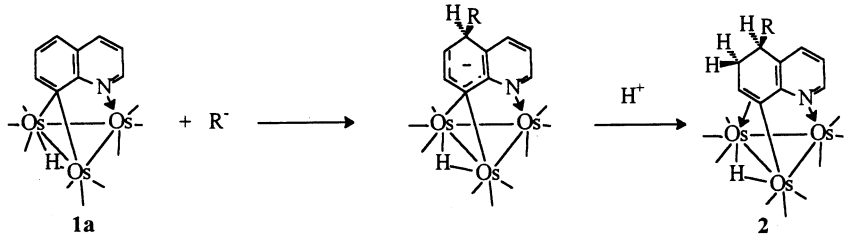

(2)

The site of nucleophilic attack in free quinolines or in η^1-N coordinated quinolines is normally the 2-position or the 4-position if the former is blocked [7,12]. Successful addition of the carbanion would allow a novel method for derivatizing the quinoline family of heterocycles on the carbocyclic ring. In light of the importance of quinolines and related benzoheterocycle ring systems in drug design and development [13], as agonists or antagonists for neurotransmitter molecules [13] and as intermediates in natural products syntheses [14] these results represent a potentially useful synthetic methodology not available via complexation by monometallic species. We report here an overview of the prior work [11] with some new examples of the reactions of quinolines with carbanions, a full discussion of the effect of substituents on the formation of complexes with bonding modes like **1a**, and the extension of the formation of this type of complex to a wide range of related benzoheterocycles.

2. Results and discussion

2.1. Reactions of carbanions with **1a**

When compound **1a** is reacted with a two- to threefold excess of the carbanions listed in Table 1 at −78°C, the nucleophilic addition products $[Os_3(CO)_9(\mu_3\text{-}\eta^3\text{-}C_9H_7(5\text{-}R')N)(\mu\text{-}H)]$ (**2a–2l**) are isolated in moderate to good yields after quenching with acid (Scheme 1). The only carbanion tried which did not result in nucleophilic addition on the ring was sodium diethylmalonate which apparently complexes with **1a** at the metal core as evidenced by the reversible color change from green to yellow when this reagent is added to **1a** at −78°C and then warmed to room temperature. This behavior, and the associated color change, is similar to that observed for the reaction of **1a** with neutral two electron donors [8–10]. Methoxide also failed to react with **1a**. It can be seen from the yields listed in Table 1 that the harder, more nucleophilic carbanions give somewhat lower yields than the softer nucleophiles. This is probably due to competing attack at the coordinated carbonyl groups, leading to decomposition. Overall, **1a** reacts with a broader range of nucleophiles relative to the neutral monometallic π-arene complexes [15]. This is undoubtedly due to localization of the electron deficiency at the 5-position resulting from the electron deficient bonding to the cluster [8–11]. Thus lithium *t*-butyl acetate reacts quite well with **1a** while in the case of $[(\pi\text{-}\eta^6\text{ arene})Cr(CO)_3]$ yields were quite low except in the presence of very polar solvents such as HMPA [15]. Methyl lithium and *n*-butyl lithium deprotonate $[(\pi\text{-}\eta^6\text{-arene})Cr(CO)_3]$ while **1a** yields the usual nucleophilic addition products [15]. Indeed, we have attempted deprotonation with lithium diisopropyl amide but observed no evidence for this mode of reaction with **1a** [11].

Table 1
Isolated nucleophilic addition product yields from the reaction of $Os_3(CO)_9(\mu_3\text{-}\eta^2\text{-}C_9H_6N)(\mu\text{-}H)$ (**1a**) with carbanions

Compound	Carbanion	Yield (%)
2a	LiMe	65
2b	Li^{n}Bu	45
2c	Li^{t}Bu	52
2d	LiBz	48
2e	LiPh	66
2f	$LiCH{=}CH_2$	51
2g	$LiC_2(CH_2)_3CH_3$	48
2h	$LiCH_2CN$	72
2i	$LiC(CH_3)_2CN$	69
2j	$Li\text{–}CHS(CH_2)_2S\text{–}$	72
2k	$LiCH_2CO_2^tBu$	86
2a	MeMgBr	43
2l	$CH_2 = CHCH_2MgBr$	53

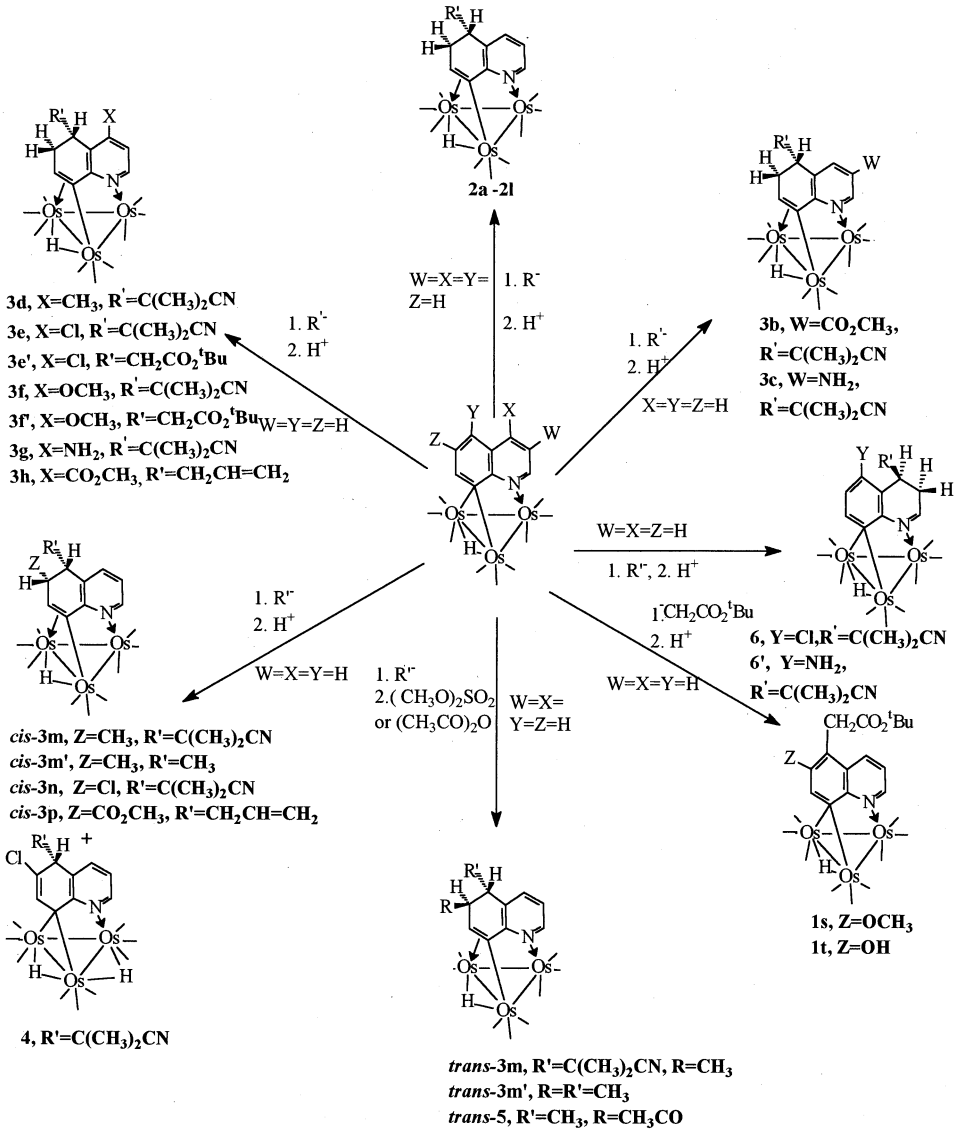

Scheme 1.

2.2. Synthesis of quinoline ring substituted analogs of **1a**

The synthesis of these electron deficient complexes can be extended to a wide range of quinolines substituted in the 3-, 4-, 5-, and 6-positions (Scheme 2) in moderate to good yields (Table 2). Substitution in the 2- or 7-positions, however, does not result in formation of the decacarbonyl precursors to complexes of structural type **1**, presumably due to steric crowding of the incipient coordination

sites at the 2- and 8-positions. Anilinic nitrogens in the 3-, 4- and 5-positions do not compete effectively with the quinoline nitrogen and reasonable yields of these analogs **1c**, **1g**, and **1l** are obtained (Table 2). However, **1l** is formed in high yield at ambient temperatures. All the compounds in Table 2 require thermolysis at $>100°C$ or photolysis in order to decarbonylate the decacarbonyl precursors to obtain the desired electron deficient species. The 5-amino derivative **1l**, has the strongly electron donating amino group in the 5-position which stabilizes the electron deficient bonding mode via accessible resonance structures (Scheme 3). This relief of electron deficiency at the metal core is also manifested by the fact that **1l** does not react with two electron donors while **1c** does; and by the fact that **1l** protonates more readily at the metal core than **1c** [10].

In the case of 3-carboxy quinoline $^{2}\eta$-N–C(8) bonding is realized but further reaction with the free carboxyl group occurs to give a complex whose ^{1}H-NMR suggests $[Os_3(CO)_9(\mu_3\text{-}\eta^3\text{-}C_9H_5(3\text{-}CO_2)N)(\mu\text{-}H)_2]$ where the carboxylic acid hydrogen has oxidatively added to the cluster. Methylation of the carboxyl group obviously blocks this secondary reaction and good yields of the desired analog, **1b**, are obtained after photolysis (Table 2). Similar results are realized for 4-carboxy quinoline and 6-carboxy quinoline methyl esters both of which give the

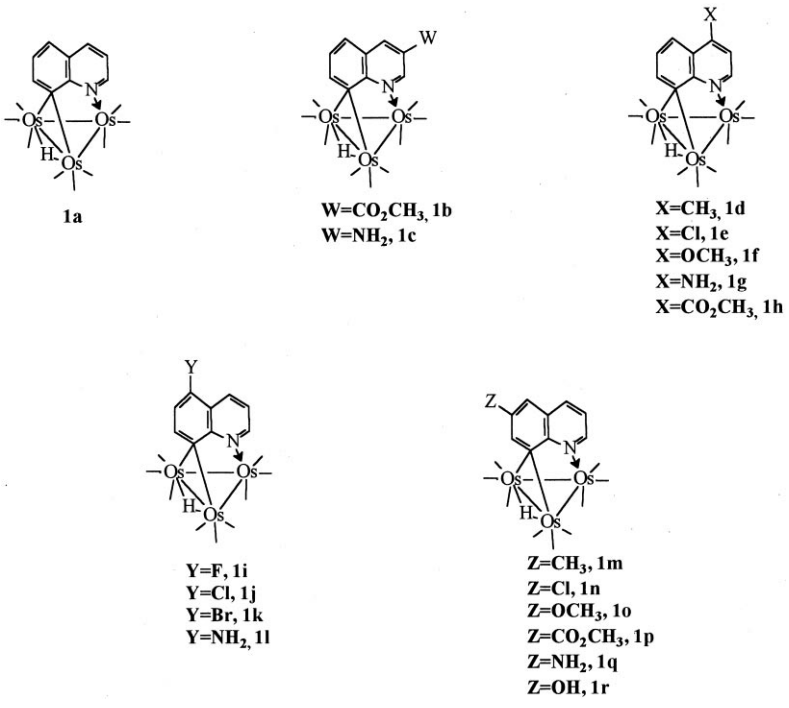

Scheme 2.

Table 2
Yields of monosubstituted electron deficient quinoline triosmium clusters [a]

Compound	Substituent	Yield (%)	Ref.
1a	H	68	[8]
1b	3-CO_2CH_3	59	This work
1c	3-NH_2	55	[10]
1d	4-CH_3	72	[8]
1e	4-Cl	76	[11]
1f	4-OCH_3	74	[11]
1g	4-NH_2	72	This work
1h	4-CO_2CH_3	40	This work
1I	5-F	70	This work
1j	5-Cl	70	[11]
1k	5-Br	80	[10]
1l	5-NH_2	82	[10]
1m	6-CH_3	84	[8]
1n	6-Cl	74	[11]
1o	6-OCH_3	56	[11]
1p	6-CO_2CH_3	61	This work
1q	6-NH_2	55	[10]
1r	6-OH	43	This work

[a] Yields are based on $Os_3(CO)_{12}$.

desired products, **1h** and **1p**, in reasonable yields (Table 2). The oxidative addition of the phenolic OH does not compete with CH oxidative addition or N coordination but does reverse the relative yields of the $^2\eta$-N–C(8) and $^2\eta$-N–C(2) products (Eq. 1) with the desired decacarbonyl product being obtained in insufficient amounts to warrant further study of the 4-hydroxy analog of **1a**. This suggests that making the heterocyclic ring very electron rich favors CH oxidative addition at C(2). This is a fairly subtle effect since the normal ratio of products is obtained with 4-methoxy quinoline and good yields are obtained for the 4-methoxy analog, **1f**, upon photolysis (Table 2). The 6-hydroxy derivative **1r**, is obtained in reasonable yield as is the 6-mehoxy derivative, **1o** [11].

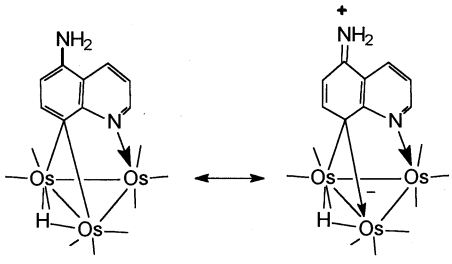

Scheme 3.

2.3. Reactions of quinoline ring substituted analogs of **1a** with carbanions

Substitution at both the carbocyclic and heterocyclic ring over a range of functional groups is well tolerated for the nucleophilic additions described above. Thus, the 3-substituted derivatives **1b** and **1c** and (Scheme 2) react with $[LiC(CH_3)_2CN]$ to give the expected nucleophilic addition products $[Os_3(CO)_9(\mu_3\text{-}\eta^3\text{-}C_9H_6(3\text{-}W)(5\text{-}R')N)(\mu\text{-}H)]$ ($W = CO_2CH_3$, $R' = C(CH_3)_2CN$ **3b**; $W = NH_2$, $R' = C(CH_3)_2CN$ **3c**; Scheme 1) in reasonable yields. Similarly, the 4-substituted derivatives **1d**–**1g** react with $[LiC(CH_3)_2CN]$ and/or $[LiCH_2CO_2^tBu]$ in an analogous manner to give $[Os_3(CO)_9(\mu_3\text{-}\eta^3\text{-}C_9H_6(4\text{-}X)(5\text{-}R')N)(\mu\text{-}H)]$ ($X = CH_3$, $R' = C(CH_3)_2CN$, **3d**; $X = Cl$, $R' = C(CH_3)_2CN$, **3e**; $R' = CH_2CO_2^tBu$, **3e′**; $X = OCH_3$, $R' = C(CH_3)_2CN$, **3f**; $X = OCH_3$, $R' = CH_2CO_2^tBu$, **3f′**; $X = NH_2$, $R' = C(CH_3)_2CN$, **3g**; Scheme 1). The 4-carboxymethyl derivative, **1h** reacts cleanly with allyl magnesium bromide to give the expected nucleophilic addition product, $[Os_3(CO)_9(\mu_3\text{-}\eta^3\text{-}C_9H_6(4\text{-}X)(5\text{-}R')N)(\mu\text{-}H)]$ ($X = CO_2CH_3$, $R' = C(CH_3)_2CN$, **3h**; Scheme 1). It is significant that in the case of the 3- and 4-carboxymethyl derivatives, attack of the carbanion at the carbonyl group represents a competitive pathway since the expected nucleophilic addition products are obtained in good yield. However, in the case of the 4-carboxy derivative only, secondary alkylation at the carbonyl group does occur in the presence excess alkylating agent (lithium isobutyronitrile or allyl magnesium bromide) with elimination of methanol to give the corresponding ketone. Also if deprotonation of the methyl and amino groups in complexes **1c**, **1e** and **1g** is occurring it does not interfere with subsequent nucleophilic addition since reasonable yields of the expected products are obtained without the need to add an increased amount of carbanion relative to **1a**.

The 6-substituted quinoline derivatives undergo nucleophilic addition as well but with interesting differences. Complex **1n** reacts with $[LiC(CH_3)_2CN]$ to give two major products, the expected nucleophilic addition product, $[Os_3(CO)_9(\mu_3\text{-}\eta^3\text{-}C_9H_6(6\text{-}Cl)(5\text{-}C(CH_3)_2CN)N)(\mu\text{-}H)]$ (**3n**) and a dihydrido complex $[Os_3(CO)_9(\mu_3\text{-}\eta^2\text{-}C_9H_5(6\text{-}Cl)(5\text{-}C(CH_3)_2CN)N)(\mu\text{-}H)_2]$ (**4**), apparently resulting from competitive protonation at the metal core (Scheme 1) [11]. We have reported the solid state structure of **4**. The formation of **4** from **1n** can be rationalized by the electron withdrawing effect of the chloride, making protonation at the 6-position less favorable and resulting in competitive protonation at the metal core [11]. To some extent, the relative amounts of **3n** and **4** can be controlled. When a tenfold excess of acid is used to quench the nucleophilic addition, **3n** and **4** are formed in a 3:2 ratio while when one equivalent of acid is used, the ratio is 5:1. This reflects the greater statistical probability for protonation at the Os_3 core relative to the C(6) position of the ring. Attempts to convert **4** to **3n** by heating at 80°C in C_6D_6 for several hours failed. In metal cluster chemistry it is not uncommon to observe the formation of two isomeric products which do not interconvert at temperatures below the decomposition temperature of the compounds [16]. The formation of **4** lends credence to our proposed structure for the intermediate anion as it is identical in structure to one of the resonance forms proposed (Eq. 2).

The reaction of **1n** with [$LiC(CH_3)_2CN$] gave only one of two possible diastereomers of **3n** (Scheme 1). The observed coupling constant between the C(5) and C(6) protons of 5.77 Hz gave no firm indication of the stereochemistry across the C(5)–C(6) bond since this value is right on the borderline between the values for *cis*- and *trans*-orientations around the C(3)–C(4) bonds in cyclohexenes [17]. In addition, the metal ligand bonding framework for structural types **2** and **3** imparts an unusual puckered geometry to the carbocyclic ring [9] which makes inferring stereochemistry from coupling constants unreliable. Unfortunately, we were unable to obtain X-ray quality crystals for **3n**.

The reaction of **1m** with [$LiC(CH_3)_2CN$] gave one major product in 71% yield, [$Os_3(CO)_9(\mu_3\text{-}\eta^3\text{-}C_9H_6(6\text{-}CH_3)(5\text{-}C(CH_3)_2CN)N)(\mu\text{-}H)$] (**3m**). This compound was also isolated as one diastereomer and showed a vicinal coupling constant for the C(5)–C(6) protons of 5.95 Hz very similar to **3n** (Scheme 1). Examination of the crude reaction mixture by ^{1}H-NMR prior to chromatographic purification showed the presence of only one diastereomer of **3m** in addition to starting material. Thus, the single diastereomer appears to be the kinetic product and is not the result of equilibration on the silica gel used for purification. The solid state structure of **3m** revealed that it exists as the *cis*-diastereomer and therefor, based on the similar vicinal coupling constants, **3n** is as well. The carbomethoxy derivative, **1p**, also gives the *cis*-isomer, **3p**, exclusively when reacted with allyl magnesium bromide in good yield (Scheme 1)

The σ-π-vinyl bonding mode is most likely undergoing a σ-π-interchange in solution as observed in related compounds [9] but it is not possible to ascertain if this process is operative owing to the asymmetry in **3m**–**3p**. The *cis*-stereochemistry can be rationalized by exclusive *trans*-protonation of an essentially planar anionic intermediate (Eq. 2), where the bulky nucleophile blocks one face of the carbocyclic ring at C(6). This is not the case for deuteride as a nucleophile where both *cis*- and *trans*-isomers are observed in similar amounts when **1m** is treated with D^-/H^+ [9]. When **1m** is reacted with $LiCH_3$, one major stereoisomer is obtained in 67% yield, [$Os_3(CO)_9(\mu_3\text{-}\eta^3\text{-}C_9H_6(5,6\text{-}CH_3)_2N)(\mu\text{-}H)$] (**3m′**), which we can identify as the *cis*-diastereomer from ^{1}H-NMR decoupling experiments which reveal a vicinal $^3J^1H\text{–}^1H = 4.5$ Hz across the C(5)–C(6) bond. A trace amount of a second diasteriomer is observed as companion peaks in the ^{1}H-NMR of **3m′**. Thus, even a relatively small alkyl group on C(5) is sufficient to induce almost exclusive *trans*-protonation.

If our hypothesis about *trans*-protonation is correct, then it should be possible to obtain *trans*-**3m** by treatment of **1a** with [$LiC(CH_3)_2CN$] followed by reaction with [$(CH_3O)_2SO_2$]. This is indeed the case (Scheme 1), although complete conversion to *trans*-**3m** is not realized, as significant amounts (ca. 40%) of **2i** are formed. Presumably, this occurs by incomplete alkylation of the anion intermediate, followed by protonation on workup with silica gel. It was not possible to separate *trans*-**3m** from **2i** by thin layer chromatography but analytically pure samples were obtained by reverse phase high pressure liquid chromatography. Although it was immediately obvious that *trans*-**3m** was a different stereoisomer than *cis*-**3**, the vicinal coupling constant across the C(5)–C(6) bond was observed to be < 1 Hz. This seemed very unusual for a *trans*-isomer, but a solid state structure determination of this product revealed that it was indeed *trans*-**3m** [11]

The same reaction sequence with **1a** using [LiMe] and [$(CH_3O)_2SO_2$] yields *trans*-**3m**′ (Scheme 1). In this case, alkylation was also incomplete and **2a** was isolated as a coproduct. The vicinal coupling constant in the case of *trans*-**3m**′ is 11.98 Hz indicating that with the smaller methyl group, the carbocyclic ring can adopt a conformation where the hydrogens are approximately *trans*-diaxial [17].

The anion generated from the treatment of **1a** with [LiMe] can also be quenched with acetic anhydride to give [*trans*-$Os_3(CO)_9(\mu_3\text{-}\eta^3\text{-}C_9H_6(5\text{-}CH_3)(6\text{-}CH_3CO)N)(\mu\text{-}H)$] (**5**) (Scheme 1). The vicinal coupling constant across the C(5)–C(6) bond is 12.12 Hz. As might be expected, the more sterically compact sp^2 carbon of the acetyl group allows the substituents on C(5) and C(6) to adopt a diequatorial conformation resulting in a *trans*-diaxial relationship for the hydrogens on these carbons as for *trans*-**3m**′.

The reaction of **1o** with [$LiCH_2CO_2^tBu$] gives the green aromatized complex [$Os_3(CO)_9(\mu_3\text{-}\eta^2\text{-}C_9H_4(6\text{-}OCH_3)(5\text{-}CH_2CO_2^tBu)N)(\mu\text{-}H)$] (**1s**, Scheme 1) in 54% yield. In addition, 35% of the corresponding phenol, [$Os_3(CO)_9(\mu_3\text{-}\eta^2\text{-}C_9H_4(6\text{-}OH)(5\text{-}CH_2CO_2^tBu)N)(\mu\text{-}H)$] (**1t**) is also isolated, probably as a result of hydrolysis by trace moisture during the acid quench or on workup on silica gel. This probably takes place prior to rearomatization from the hydrolytically sensitive allyl ether intermediate. The facile oxidation (dehydrogenation) of the intermediate nucleophilic addition product is a result of the presence of the strongly π-electron donating 6-methoxyl group and the alkyl substituent in the 5-position. Small amounts of rearomatized products were also noted in the reactions of **1m** with [LiMe] and [$LiC(CH_3)_2CN$]. Consistent with this idea is the fact that the 6-carboxymethyl derivative **1p**, forms the expected nucleophilic addition product [$Os_3(CO)_9(\mu_3\text{-}\eta^3\text{-}C_9H_6(5\text{-}CH_2CH{=}CH_2)(6\text{-}CO_2CH_3)N)(\mu\text{-}H)$] (**3p**, Scheme 1), without the accompanying rearomatization on reaction with allyl magnesium bromide in good yield.

The highly regioselective nature of the nucleophilic additions observed for structural type **1** regardless of the nature or location of the substituents on the quinoline ring poses the question as to what would occur if the 5-position were substituted with a reasonable leaving group. In the case of halide substituted $\pi\text{-}\eta^6$ arene complexes, nucleophilic substitution competes with nucleophilic addition [15]. The reaction of the 5-chloro derivative **1j** (Scheme 2) with [$LiC(CH_3)_2CN$] results in nucleophilic addition across the 3,4-bond of the quinoline ring to yield [$Os_3(CO)_9(\mu_3\text{-}\eta^2\text{-}C_9H_6(5\text{-}Cl)(4\text{-}C(CH_3)_2\text{-}CN)N)(\mu\text{-}H)$] (**6**, Scheme 1). The ^{1}H-COSY NMR of **6** clearly shows the coupling of the most downfield aromatic resonance (i.e. C(2)–H) resonance coupled to the most upfield aliphatic resonances and two separately coupled aromatic resonances. These data are consistent with the structure shown in Scheme 1 and this has been verified by a solid state structure determination of this complex [11]. The reaction of the 5-amino derivative, **1l**, with [$LiC(CH_3)_2CN$] yields the analogous nucleophilic addition product [$Os_3(CO)_9(\mu_3\text{-}\eta^2\text{-}C_9H_6(5\text{-}NH_2)(4\text{-}C(CH_3)_2\text{-}CN)N)(\mu\text{-}H)$] (**6**′, Scheme 1) and similar results are realized with **1i** and **1k**.

2.4. Rearomatization of the nucleophilic addition products

The facile rearomatization of the nucleophilic addition product derived from the addition of [$LiCH_2CO_2^tBu$] to **1o** (Scheme 1) prompted us to attempt to reproduce this process in a deliberate manner. There are several methods which proved adequate.

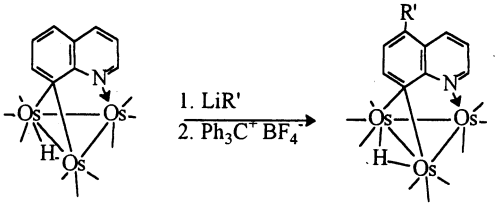

(3)

1a

1u, R' = n-Bu
1v, R' = $CH_2CO_2^tBu$

The addition of the trityl cation to the anion resulting from the addition of alkylating agents [R′Li] (R′ = *n*-Bu, $CH_2CO_2^tBu$) to **1a** gave the rearomatized products [$Os_3(CO)_9(\mu_3\text{-}\eta^2\text{-}C_9H_5(5\text{-}R')N)(\mu\text{-}H)$] (**1u**, R′ = ^{n}Bu; R = **1v**, $CH_2CO_2^tBu$; Eq. 3) in 53 and 83% yield, respectively. In some other cases, we found the coproduct, triphenyl methane difficult to separate from the products. An alternative route is the addition of dichlorodicyanoquinone (DDQ) followed by an ethanol quench of the resulting hydroquinone anion and excess carbanion. Thus, **1m** is treated with $LiCH_3$ then DDQ/EtOH) to yield [$Os_3(CO)_9(\mu_3\text{-}\eta^2\text{-}C_9H_4(5,6\text{-}CH_3)_2)N)(\mu\text{-}H)$] (**1w**, Eq. 4). Finally, one can add a deprotonating agent such as diazabicyclononane (DBU) to the isolated nucleophilic addition products of type **2** or **3** followed by DDQ/EtOH, as demonstrated with **2a**, which yielded [$Os_3(CO)_9(\mu_3\text{-}\eta^2\text{-}C_9H_5(5\text{-}CH_3)N)(\mu\text{-}H)$] (**1x**) (Eq. 5). Attempts to react **2** or **3** with DDQ directly failed. Choosing the best route from among these methods remains uncertain at present except to say that DDQ seems to tolerate functionality a bit better and its reaction products are easier to separate from the cluster reaction products. In cases where multiple products result, isolation of the nucleophilic addition product followed by DBU/DDQ treatment would be the method of choice.

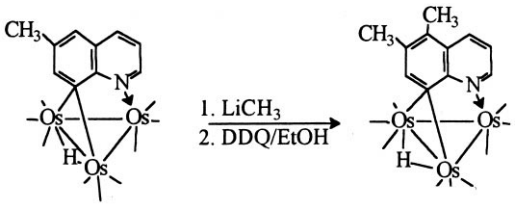

(4)

1m

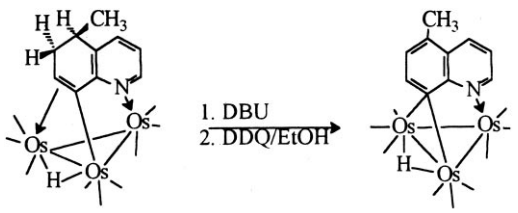

(5)

2a **1x**

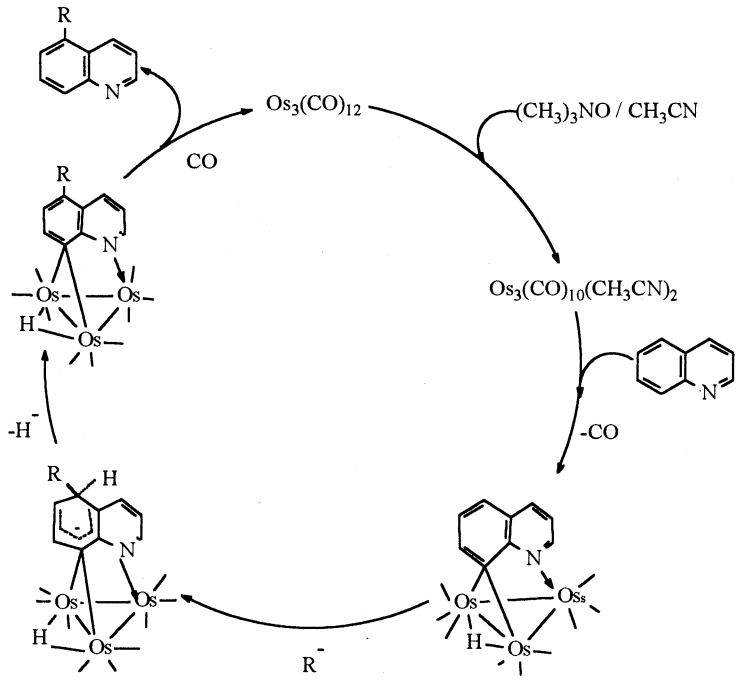

Scheme 4.

2.5. Cleavage of the functionalized quinoline from the cluster

In order for this synthetic methodology to be developed as a useful tool for the synthesis of novel quinoline derivatives, a clean method for cleavage of the quinoline ligand from the cluster is required. For the rearomatized derivatives of structural type **1** this method proved to be heating the quinoline cluster complex at 70°C in acetonitrile under an atmosphere of carbon monoxide. This leads to isolation of the free quinoline and formation of $Os_3(CO)_{12}$. The $[Os_3(CO)_{12}]$ precipitates almost quantitatively from the cooled reaction solution while the quinoline can be recovered by evaporation of solvent and filtration through silica if necessary. Including the aromatization procedures outlined above, successful cleavage by this method constitutes a stoichiometric cycle for selectively alkylating quinolines at the 5-position (Scheme 4). Unfortunately, this method does not extend to the nucleophilic addition products of structural types **2** or **3**. Although cleavage is observed at elevated pressures of carbon monoxide, the reaction is not clean resulting in a mixture of products. Other approaches to cleaving these ligands are currently being explored.

2.6. Extension to other heterocycles

It would appear from the above results that any heterocycle containing a pyridine like nitrogen β- to a CH bond of a fused benzene ring should be able to form the same bonding mode as observed for structural type **1** and thus result in the carbon atom *para*- to this CH bond activated towards nucleophilic addition/substitution. The obvious importance of this class of molecules prompted us to explore the generalization of Eq. 1 to these heterocycles.

The most obvious extension is to the tricyclic analogs of quinoline. Thus phenanthridine and 5,6-benzoquinoline both react with $[Os_3(CO)_{10}(CH_3CN)_2]$ to give the decacarbonyl precursors desired which on photolysis convert to the structural analogs of **1**, $[Os_3(CO)_9(\mu_3\text{-}\eta^2\text{-}C_{13}H_8N)(\mu\text{-}H)]$ (**7** and **8**, respectively; Table 3, Eqs. 6 and 7).

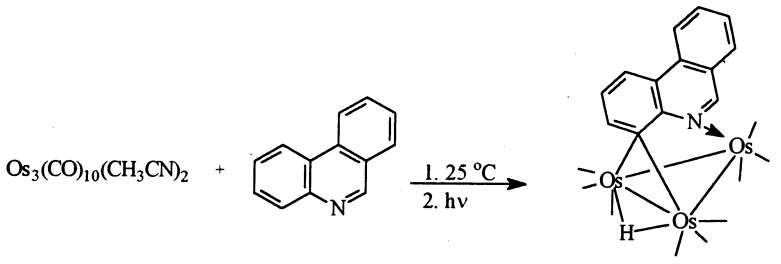

(6)

7

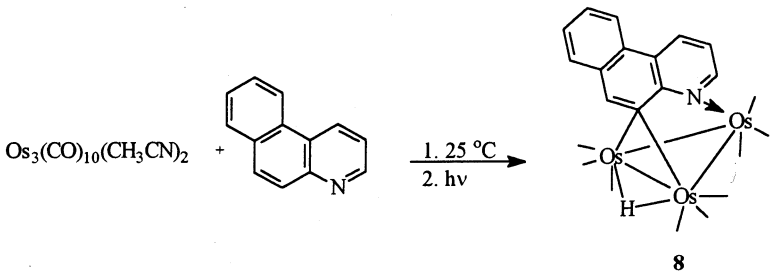

(7)

8

Table 3
Isolated yields of electron deficient benzoheterocycle triosmium clusters [a]

Compound	Heterocycle	Yield
7	Phenanthradine	43
8	5,6-Benzoquinoline	54
9	2-Methyl benzimidazole	35
10	2-Methyl benzotriazole	32
11	2-Methyl benzoxazole	55
12	Benzothiazole	36
13	2-Methyl benzothiazole	34
14	Quinoxaline	55

[a] Yields are based on osmium carbonyl.

The family of five-membered heterocycles containing two heteroatoms and a fused benzene ring is another obvious series to explore. Indeed, the reaction of benzimidazole and benzotriazole with $[Os_3(CO)_{10}(CH_3CN)_2]$ has been reported but the major product is the result of CH or NH activation at the 2-position [18,19]. However, if 2-methyl benzimidazole or 2-methyl benzotriazole are used the major product is the decacarbonyl which is the result of CH activation at C(7) which cleanly decarbonylate on photolysis to the structural analogs of **1** in reasonable yield, $[Os_3(CO)_9(\mu_3\text{-}\eta^2\text{-}(2\text{-}CH_3)C_6H_4N_2X)(\mu\text{-}H)]$ (X = C, **9**; X = N, **10**; Table 3, Eq. 8).

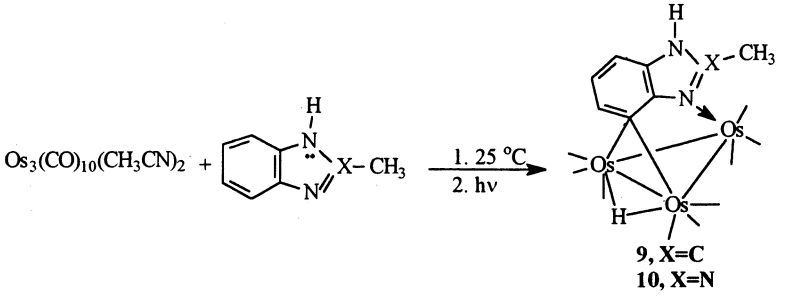

(8)

The related heterocycles 2-methyl-benzoxazole, benzothiazole and 2-methyl benzothiazole all give the desired CH activation at C(7) and the corresponding analogs of **1** after photolysis, $[Os_3(CO)_9(\mu_3\text{-}\eta^2\text{-}(2\text{-}R)C_6H_3NCX)](\mu\text{-}H)]$ (X = O, R = H, **11**; X = S, R = H **12**; X = S, R = CH_3, **13**; Table 3, Eq. 9). There is apparently a relationship between the aromaticity of the heterocyclic ring and the relative reactivity of the C(2) which is also seen in the monocyclic counterparts of these ligands [20].

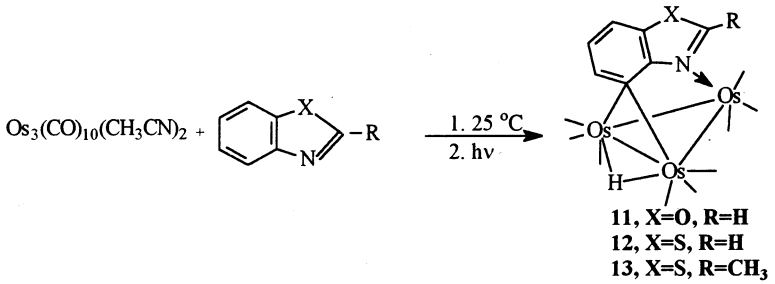

(9)

Finally, quinoxaline reacts with $[Os_3(CO)_{10}(CH_3CN)_2]$ to give the analog of **1**, $[Os_3(CO)_9(\mu_3\text{-}\eta^2\text{-}C_8H_5N_2)(\mu\text{-}H)]$ (**14**; Table 3, Eq. 10) after photolysis, in good yield. In order to avoid formation of what appeared to be a 2:1 cluster to ligand complex it was necessary to use a larger excess of ligand. The isomeric heterocycles quinazoline and chinoline do not yield structural analogs of **1** giving CH activation at C(2) and an η^2-N,N bound complexes, respectively.

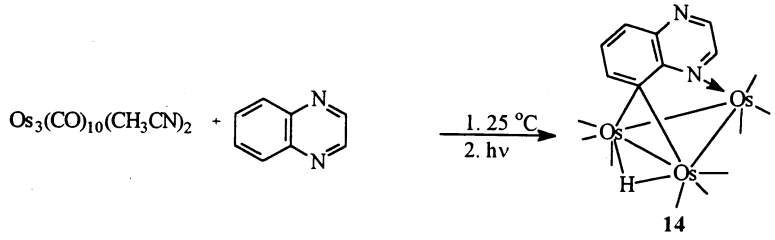

(10)

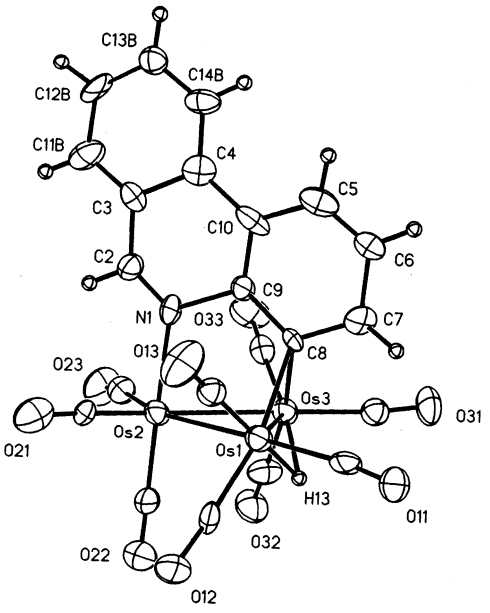

Fig. 1. Solid state structure of $Os_3(CO)_9(\mu_3\text{-}\eta^2\text{-}C_{13}H_8N)(\mu\text{-}H)$ (**7**) showing the calculated positions of the hydride.

2.7. Comparison of the solid state structures of ***7–10****,* ***12*** *and* ***1***

The synthesis of this series of electron deficient triosmium clusters, **7–14** provides the opportunity to evaluate the effect of varying the nature of the heterocycle on the metal ligand bonding framework as well as the impact of the cluster on the intraligand bond lengths. The solid state structures of complexes **7–10**, **12** and **14** are shown in Figs. 1–6, crystal data are given in Tables 4 and 5 and a comparison of relevant bond lengths are given in Table 6. The most remarkable aspect of this series of structures is the almost identical nature of the ligand–metal cluster interactions. Thus with the exception of **8** all of the three-center two-electron bonds with the Os(1)–Os(3) edge show highly symmetrical Os–C bonds with an average length of 2.26(2)–2.31(2) Å (Table 6). Compound **8** shows an asymmetry greater than three standard deviations and is also the only complex that does not show a C(5)–C(6) or C(4)–C(5) bond shorter than the average C–C bond of the metal bound carbocyclic ring (Table 6). A short C(5)–C(6) bond (1.29(3) Å) is also observed for **1a**. These data suggest that the electron deficiency normally localized at the 5-position of the quinoline ring may be delocalized into the carbocycle not bound to the metal in the case of **8**. This is indeed reflected in the chemistry of **8** where nucleophilic attack is observed on this ring [21]. The N(1)–C(2) bonds are all in the range of a localized N–C bond, again with the exception of **8**, while **7** shows

an anomalously short N–C bond. These data are more difficult to understand in light of the atomic and structural differences in the compositions of the heterocyclic rings. Given the essentially perpendicular orientation of the ring, relative to the cluster, in all of these complexes and the average bond lengths of the carbocyclic rings it is certain that these heterocycles are only involved in σ-interactions with the metal core.

3. Conclusions

The three-center two-electron bonding of the C(8) carbon of the quinoline ring with two metal atoms of the Os_3 triangle imparts a significant electron deficiency to C(5) of the quinoline ring making it subject to regiospecific attack by a wide range of carbanions. In sharp contrast to the π-η^6-chromium arenes, we do not observe lithiation with [LiMe] or [Li^{n}Bu] [15]. Substitution is not observed in the case of the 5-halo quinoline derivatives while for the π-η^6-arene complex, substitution is competitive with nucleophilic addition for most nucleophiles with halogen substituted arenes [15]. Substitution of halogen at the 5-position redirects nucleophilic attack to the 4-position resulting in nucleophilic addition across the 3,4 double bond after acid quench.

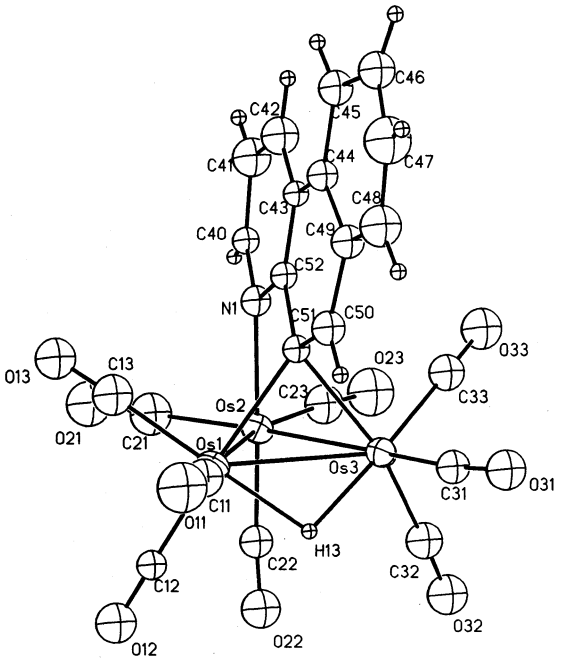

Fig. 2. Solid state structure of [$Os_3(CO)_9(\mu_3$-η^2-$C_{13}H_8N)(\mu$-H)] (**8**) showing the calculated position of the hydride.

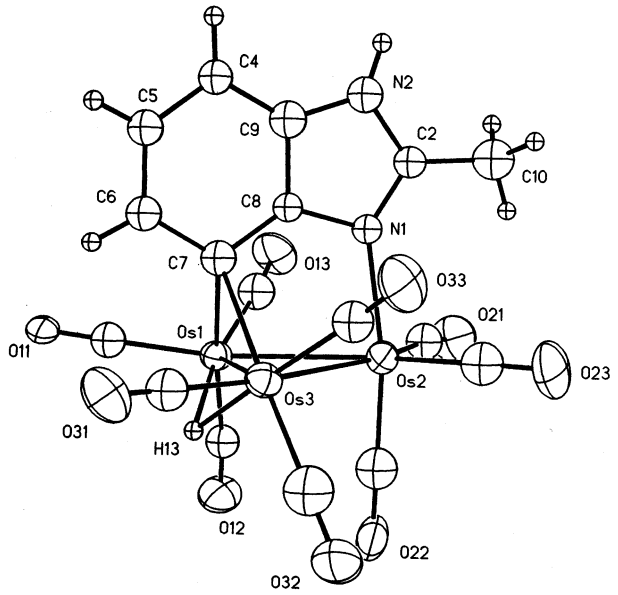

Fig. 3. Solid state structure of $[Os_3(CO)_9(\mu_3\text{-}\eta^2\text{-}C_7H_4(2\text{-}CH_3)N_2)(\mu\text{-}H)]$ (**9**) showing the calculated position of the hydride.

These results suggest that the electron deficiency is concentrated at the 5-position (and presumably the 7-position which is apparently sterically blocked). The failure to observe lithiation even with small relatively hard carbanions probably reflects this concentration of the electron deficiency whereas in the π-coordinated arenes, the electron withdrawing effect of the metal is distributed among all six carbon atoms. That substitution for halogens is a less accessible pathway for these quinoline derivatives than for $\pi\text{-}\eta^6$ arenes is more difficult to rationalize but may be due to the fact that the direction of electron polarization is along the reaction coordinate for substitution in the case of the $\pi\text{-}\eta^6$ arenes while this is not the case for the $\mu_3\text{-}\eta^2$ quinoline complexes.

It is also noteworthy that these quinoline derivatives react reasonably well with methyl and allyl Grignard reagents while the $\pi\text{-}\eta^6$ arenes do not. This is probably also related to the concentration of the electron deficiency, as described above. In addition, this may be a consequence of the fact that one might expect that the carbonyl ligands on the osmium cluster may be less subject to competitive nucleophilic attack than the carbonyls in the $\pi\text{-}\eta^6$ chromium arenes owing to their higher average infrared stretching frequencies and/or force constants of the C–O carbonyl ligand bonds [22]. Nucleophilic attack at carbomethoxy substituents on the quinoline ring and deprotonation of methyls or amines also do not compete with regioselective attack at the 5-position.

The strictly *trans*-addition of the electrophiles (H^+, CH_3^+, CH_3CO^+) is a consequence of the planar structure of the intermediate anion (Eq. 2, Scheme 1).

What is a bit surprising here is that even with the relatively small methyl group *trans*-addition is $>95\%$ by ^{1}H-NMR while with hydride as the nucleophile and proton as the electrophile, the stereoselectivity is completely lost, with both *cis*- and *trans*-addition taking place to about the same extent [9]. These results indicate that the stereoselectivity is steric in origin rather than being directed by prior coordination of the electrophile to the metal core or the carbonyl ligands. Complex **4** does not convert to **3d**, which is consistent with this interpretation. In the case of π-η^6 arene complexes quenching with electrophiles other than protons leads primarily to electrophilic alkylation of the carbanion owing to the reversibility of the nucleophilic addition [15]. We see no evidence for reversible addition in the reaction of **1** with nucleophiles although 2:3-fold excesses of the carbanions were sometimes necessary to drive the reactions to completion. Stereoselective *trans*-acylation is observed for π-η^6 arenes with methyl iodide as the electrophile in the presence of carbon monoxide and in this case, interaction with the carbonyl ligands on chromium directs the *trans*-addition [15]. Topside attack of both nucleophile and electrophile to give overall *cis*-addition is observed in the nucleophilic additions across the 5,6-bond of π-η^6 dihydro-napthyl chromium tricarbonyls [23].

Overall, there are distinct steric and electronic differences between the activation of quinolines by the μ_3-η^2 bonding mode to triosmium clusters and the well known π-η^6 arene complexes. Of course, none of this chemistry would be possible without the presence of the third metal atom which coordinates the nitrogen lone pair and apparently blocks attack at the 2-position, the normal site of nucleophilic attack in quinolines [11]. Given the wide range of heterocycles reported here which form the

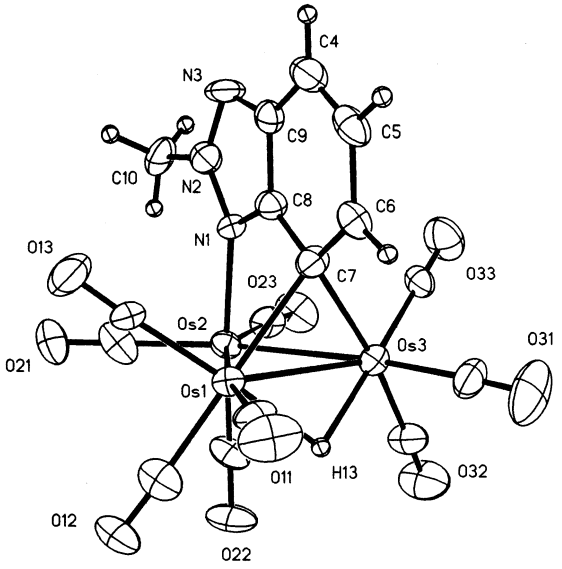

Fig. 4. Solid state structure of $[Os_3(CO)_9(\mu_3\text{-}\eta^2\text{-}C_6H_3N_3)(\mu\text{-}H)]$ (**10**) showing the calculated position of the hydride.

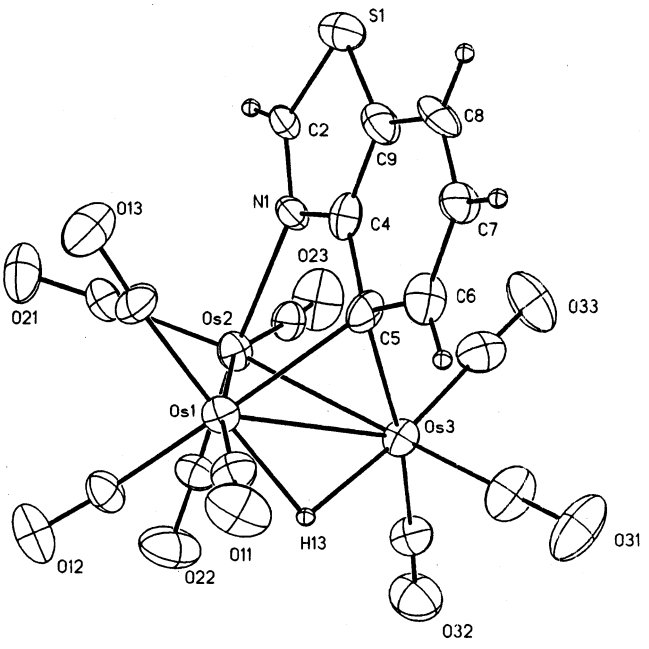

Fig. 5. Solid state structure of $[Os_3(CO)_9(\mu_3\text{-}\eta^2\text{-}C_6H_4NS)(\mu\text{-}H)]$ (**12**) showing the calculated position of the hydride.

electron deficient bonding mode with the triosmium core, the synthetic methodology outlined here for quinoline should prove useful for derivatizing the carbocyclic ring in these systems in new ways for the synthesis of compounds of interest to the biomedical community. This work is currently underway in our laboratories.

4. Experimental

All reactions were carried out under an atmosphere of nitrogen but were worked up in air. THF was distilled from benzophenone ketyl, methylene chloride and acetonitrile from calcium hydride.

IR spectra were recorded on a Perkin–Elmer 1600 FTIR spectrometer and ^{1}H- and ^{13}C-NMR were recorded on a Varian Unity Plus 400. Elemental analyses were performed by Schwarzkopf Microanalytical Labs, Woodside, New York. Chemical shifts are reported downfield positive relative to tetramethylsilane and coupling constants are reported only for those resonances relevant to the stereochemistry, while only the multiplicities of resonances with standard couplings are reported. Proton NMR assignments were made with the aid of 2D-COSY experiments.

Osmium carbonyl was purchased from Strem Chemicals, used as received and converted to $[Os_3(CO)_{10}(CH_3CN)_2]$ by published procedures [24]. Quinoline was purchased from Aldrich Chemicals, and distilled from calcium hydride before use.

The 3-, 4-, and 6-carboxy quinolines were purchased from Aldrich Chemicals and converted to their corresponding methyl esters by reflux in acidified (10 M excess sulfuric acid) followed by neutralization and ether extraction. The resulting esters were identified and analyzed for purity by ^{1}H-NMR. The 5-fluoro [25] and 4-amino [26] quinolines were prepared according to literature procedures. 6-Hydroxy quinoline was purchased from Aldrich Chemicals. DDQ and trityl tetrafluoroborate were purchased from Aldrich Chemicals, and used as received. Trifluoroacetic acid and diisopropylamine were purchased from Aldrich Chemicals, and distilled from phosphorus pentoxide and calcium hydride, respectively, before use. The carbanion reagents [Li^{n}Bu] and [allylMgBr] were purchased from Aldrich and used as received. The isobutyryl carbanion was generated by deprotonation of isobutyryl nitrile with lithium diisopropyl amide which was generated from diisopropyl amine and [Li^{n}Bu] according to published procedures [3]. Compounds **1a**, **1c**–**1f**, **1j**–**1o**, **1q**, and **1s**–**1x** were previously reported [8–11]. Compounds **2a**–**2l**, **3c**, **3e**, **3e′**, **3f**, **3f′**, *cis*- and *trans*-**3m** and **3m′**, *cis*-**3n** and **4**–**6** were also previously reported [11].

*4.1. Preparation of [Os$_3$(CO)$_9$(μ_3-η^2-C$_9$H$_5$(R)N)(μ-H)] (R = 3-CO$_2$CH$_3$, **1b**; R = 4-NH$_2$, **1g**; R = 4-CO$_2$CH$_3$, **1h**; R = -5-F, **1l**; R = 6-CO$_2$CH$_3$, **1p**; R = 6-OH, **1r**) and 7–14*

The following procedure was used for synthesizing all of the above substituted quinoline triosmium complexes as well as **7**–**14**. [$Os_3(CO)_{10}(CH_3CN)_2$ (0.250–0.500 g, 0.27–0.54 mmol)] was dissolved in 150–300 ml CH_2Cl_2 and a twofold molar

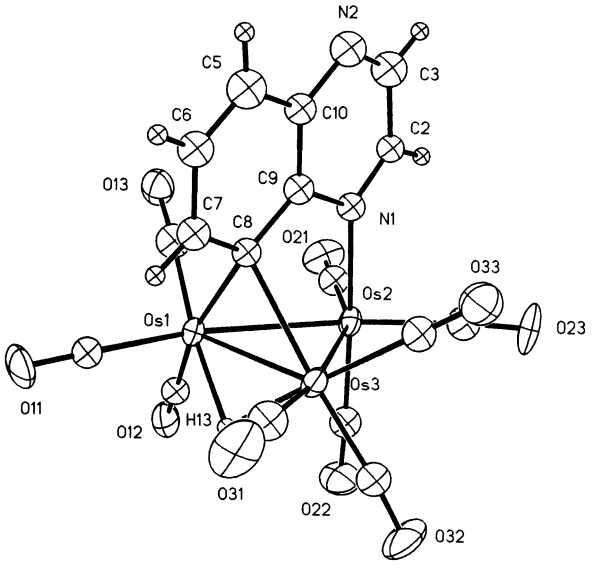

Fig. 6. Solid state structure of [$Os_3(CO)_9(\mu_3$-η^2-$C_8H_5N_2)(\mu$-H)] (**14**) showing the calculated position of the hydride.

Table 4
Crystal data and structure refinement for **7–9**

Compound	**7**	**8**	**9**
Empirical formula	$C_{22}H_9NO_9Os_3$	$C_{22}H_9NO_9Os_3$	$C_{17}H_8N_2O_9Os_3$
Formula weight	1001.90	1001.90	954.85
Temperature (K)	293(2)	293(2)	293(2)
Wavelength (Å)	0.71073	0.71073	0.71073
Crystal system	Monoclinic	Monoclinic	Monoclinic
Space group	$P2_1/n$	$P2_1/n$ (no. 14)	$P2_1/n$
Unit cell dimensions			
a (Å)	9.367(4)	10.463(2)	13.690(4)
b (Å)	17.048(4)	18.425(4)	21.652(7)
c (Å)	14.591(5)	12.201(2)	14.202(6)
α (°)	90	90	90
β (°)	94.96(3)	94.00(3)	95.21(3)
γ (°)	90	90	90
Volume (Å^3)	2321(1)	2346.4(8)	4192(2)
Z	4	4	8
D_{calc} (Mg m^{-3})	2.867	2.836	3.026
Absorption coefficient (mm^{-1})	16.434	16.258	18.192
F(000)	1792	1792	3392
Crystal size (mm)	$0.575 \times 0.200 \times 0.125$	$0.30 \times 0.15 \times 0.03$	$0.50 \times 0.10 \times 0.050$
θ Range for data collection (°)	1.84–24.98	2.01–25.00	1.72–20.00
Limiting indices	$-11 \le h \le 11$, $0 \le k \le 20$, $-17 \le l \le 17$	$-12 \le h \le 12$, $0 \le k \le 21$, $-14 \le l \le 14$	$-13 \le h \le 13$, $0 \le k \le 20$, $-13 \le l \le 13$
Reflections collected	8503	8542	8355
Independent reflections	3994 [$R_{int} = 0.249$]	4125 [$R_{int} = 0.084$]	3909 [$R_{int} = 0.0544$]
Absorption correction	ψ	ψ	None
Max./min. transmission	0.5455, 0.0464	0.9977, 0.5206	
Refinement method	Full-matrix least-squares on F^2	Full-matrix least-squares on F^2	Full-matrix least-squares on F^2
Data/restraints/parameters	3991/0/306	4125/0/201	3909/0/371
Goodness-of-fit on F^2	1.047	0.876	1.001
Final R indices [$I > 2\sigma(I)$]	$R_1 = 0.1062$, $wR_2 = 0.2687$	$R_1 = 0.0557$, $wR_2 = 0.0924$	$R_1 = 0.0471$, $wR_2 = 0.0838$
R indices (all data)	$R_1 = 0.1234$, $wR_2 = 0.2931$	$R_1 = 0.1177$, $wR_2 = 0.1243$	$R_1 = 0.0921$, $wR_2 = 0.1000$
Largest difference peak and hole (e Å^{-3})	4.551 and −4.326	1.793 and −1.282	0.878 and −0.795

excess of the appropriate heterocyclic ligand was added (except in the case of quinoxaline where better yields were obtained using a fivefold molar excess). The reaction mixture was stirred for 12–20 h and then filtered through a short silica gel column to remove excess ligand. The yellow–green reaction solution was collected in a 500 ml quartz reaction vessel and irradiated in a Rayonet photoreaction chamber for 2–4 h until no further conversion was detected by analytical TLC. In the case of compounds **7–14** it was necessary to isolate the pure decacarbonyl

precursors by preparative TLC (the slowest moving yellow–orange band) before photolysis or poorer yields were obtained. The dark green solutions obtained after photolysis were then filtered through a short silica gel column concentrated to 50–150 ml, and cooled to −20°C to yield 100–300 mg of dark green crystals. The mother liquor was rotary evaporated and taken up in a minimum amount of CH_2Cl_2 and eluted on 0.1 × 20 × 40 cm silica gel TLC plates using CH_2Cl_2/hexane (20–70% CH_2Cl_2) as the eluent. Three bands were eluted. The faster moving two

Table 5
Crystal data and structure refinement for **10**, **12** and **14**

Compound	**10**	**12**	**14**
Empirical formula	$C_{16}H_7N_3O_9Os_3$	$C_{16}H_5NO_9Os_3S$	$C_{17}H_6N_2O_9Os_3$
Formula weight	955.85	957.87	952.84
Temperature (K)	293(2)	293(2)	293(2)
Wavelength (Å)	0.71073	0.71073	0.71073
Crystal system	Monoclinic	Monoclinic	Monoclinic
Space group	$P2_1/c$	$P2_1/c$	$P2_1/c$
Unit cell dimensions			
a (Å)	8.607(4)	8.670(2)	8.588(4)
b (Å)	16.830(9)	16.614(6)	16.721(6)
c (Å)	14.628(5)	14.365(4)	14.577(6)
α (°)	90	90	90
β (°)	99.19(3)	9.87(2)	98.79(4)
γ (°)	90	90	90
Volume, Z	2092(2) Å^3, 4	2039(1) Å^3, 4	2068.7(15) Å^3, 4
D_{calc} (Mg m^{-3})	3.035	3.121	3.059
Absorption coefficient (mm^{-1})	18.232	18.804	18.433
F(000)	1696	1696	1688
Crystal size (mm)	0.70 × 0.50 × 0.33	0.38 × 0.13 × 0.12	0.35 × 0.20 × 0.10
θ Range for data collection (°)	1.86–24.98	1.89–23.9	1.87–24.97
Limiting indices	$-10 \le h \le 10$, $0 \le k \le 19$, $-17 \le l \le 17$	$-9 \le h \le 9$, $0 \le k \le 18$, $-16 \le l \le 16$	$-10 \le h \le 10$, $0 \le k \le 19$, $-17 \le l \le 17$
Reflections collected	7741	6616	7713
Independent reflections	3675 [$R_{int} = 0.1053$]	3184 [$R_{int} = 0.0480$]	3636 [$R_{int} = 0.0991$]
Absorption correction	ψ	ψ	ψ
Max./min. transmission	0.2542, 0.1320	0.378, 0.205	0.7509, 0.2106
Refinement method	Full-matrix least-squares on F^2	Full-matrix least-squares on F^2	Full-matrix least-squares on F^2
Data/restraints/parameters	3675/0/281	3184/0/272	3635/0/185
Goodness-of-fit on F^2	1.025	1.151	1.063
Final R indices [$I > 2\sigma(I)$]	$R_1 = 0.0661$, $wR_2 = 0.1571$	$R_1 = 0.0383$, $wR_2 = 0.0585$	$R_1 = 0.0587$, $wR_2 = 0.1296$
R indices (all data)	$R_1 = 0.0783$, $wR_2 = 0.1682$	$R_1 = 0.0576$, $wR_2 = 0.0626$	$R_1 = 0.0793$, $wR_2 = 0.1412$
Extinction coefficient	0.0045(3)	0.00073(3)	
Largest difference peak and hole (e Å^{-3})	5.682 and −2.740	0.852 and −0.744	4.334 and −2.508

Table 6
Selected distances (Å) for compounds **7**–**10**, **12** and **14** [a]

Compound	C–Os(1)	C–Os(3)	N(1)–Os(2)	C–C Av. Carbocycle(s) [b]	N(1)–C(2)	C(5,4)–C(6,5) [c]	Av. Os–CO
7	2.29(2)	2.25(3)	2.17(2)	1.41(4) (1.35(4))	1.19(3)	1.32(5)	1.89(3)
8	2.22(1)	2.32(1)	2.13(1)	1.42(1) (1.41(1))	1.45(1)	1.35(1)	1.89(1)
9	2.27(2)	2.26(3)	2.15(2)	1.39(3)	1.31(3)	1.36(3)	1.88(1)
10	2.31(2)	2.29(2)	2.14(1)	1.39(3)	1.29(3)	1.35(3)	1.90((2)
12	2.27(1)	2.25(1)	2.14(1)	1.38(2)	1.30(1)	1.35(1)	1.88(2)
14	2.30(2)	2.32(2)	2.10(1)	1.37(3)	1.26(3)	1.31(3)	1.89(2)

[a] Numbers following each entry in parentheses are the average standard deviations.
[b] The average bond lengths of the carbocyclic ring not bound to the metal are given in parentheses.
[c] Refers to either the C(5)–C(6) or C(4)–C(5) bond lengths in **7**, **8** and **14** and **9**, **10** and **12**, respectively.

yellow bands contained minor amounts of the decacarbonyl quinoline triosmium complexes and the slower moving dark green band contained additional product which was crystallized from methylene chloride hexanes. The combined total yields (based on $Os_3(CO)_{12}$) of the products are listed in Tables 2 and 3 and the analytical and spectroscopic data are given below.

Compound **1b**: Anal. Calc. for $C_{20}H_9NO_{11}Os_3$: C, 23.76; H, 0.99; N, 1.38. Found: C, 23.52; H, 0.82; N, 1.40%. IR (ν CO) in CH_2Cl_2: 2078 s, 2050 s, 2022 s, 1994 br, 1954 w cm^{-1}. ^{1}H-NMR of **1b** at 400 MHz in $CDCl_3$: δ 9.74 (s, H(2)), 8.69 (s, H(4)), 8.66 (dd, H(5)), 8.48 (dd, H(7)), 7.28 (t, H(6)), 4.04 (s, CH_3), −12.06 (s, hydride).

Compound **1g**: yield for **1g**: 72.2%. Anal. Calc. for $C_{18}H_8N_2O_9Os_3$: C, 22.34; H, 0.83; N, 2.89. Found: C, 21.07; H, 0.79; N, 2.58%. IR (ν CO) in CH_2Cl_2: 2078 s, 2050 s, 2022 s, 1994 br, 1954 w cm^{-1}. ^{1}H-NMR of **1g** at 400 MHz in CD_3COCD_3: δ 9.09 (s, H(2)), 8.81 (d, H(5)), 8.65 (dd, H(3)), 7.46 (s br, NH_2), 7.23 (t, H(6)), 6.48 (d, H(7)), −12.07 (s, hydride).

Compound **1h**: yield for **1h**: 40.3%. Anal. Calc. for $C_{20}H_9NO_{11}Os_3$: C, 23.76; H, 0.99; N, 1.38. Found: C, 23.14; H, 0.88; N, 1.35%. IR (ν CO) in CH_2Cl_2: 2078 s, 2050 s, 2022 s, 1994 br, 1954 w cm^{-1}. ^{1}H-NMR of **1h** at 400 MHz in $CDCl_3$: δ 9.45 (d, H(2)), 9.41 (d, H(5)), 8.62 (d, H(7)), 7.56 (t, H(3)), 7.28 (t, H(6)), 4.02 (s, CH_3), −12.24 (s, hydride).

Compound **1i**: Anal. Calc. for $C_{18}H_6NO_9FOs_3$: C, 22.27; H, 0.61; N, 1.44. Found: C, 22.83; H, 0.81; N, 1.56%. IR (ν CO) in CH_2Cl_2: 2076 s, 2050 s, 2026 s, 1996 m, 1980 m, 1962 w, 1948 w cm^{-1}. ^{1}H-NMR of **1i** at 400 MHz in $CDCl_3$: δ 9.32 (dd, H(2)), 8.65 (d, H(6)), 8.32 (dd, H(4)), 7.16 (dd, H(7)), 6.95 (t, H(3)), −12.20 (s, hydride).

Compound **1p**: Anal. Calc. for $C_{20}H_9NO_{11}Os_3$: C, 23.76; H, 0.99; N, 1.38. Found: C, 23.70; H, 1.04; N, 1.57%. IR (ν CO) in CH_2Cl_2: 2079 s, 205 s, 2023 s, 1994 br, 1954 w cm^{-1}. ^{1}H-NMR of **1p** at 400 MHz in $CDCl_3$: δ 9.32 (dd, H(2)), 9.02 (s, H(5)), 8.93 (s, H(7)), 8.12 (dd, H(4)), 7.17 (t, H(3)), 4.01 (s, CH_3), −12.06 (s, hydride).

Compound **1r**: Anal. Calc. for $C_{18}H_7NO_{10}Os_3$: C, 22.34; H, 0.72; N, 1.45. Found: C, 21.99; H, 0.75; N, 1.41%. IR (ν CO) in CH_2Cl_2: 2076 m, 2058 s, 2047 s, 2018 s, 1990 s, br, 1941 w, br cm^{-1}. ^{1}H-NMR of **14** at 400 MHz in $CDCl_3$: δ 9.08 (d, H(2)), 8.15 (d, H(7)), 7.91 (d, H(4)), 7.71 (d, H(5)), 7.05 (dd, H(3)), 6.01 (br, OH), −12.07 (s, hydride).

Compound **7**: Anal. Calc. for $C_{22}H_9NO_9Os_3$: C, 26.37; H, 0.90; N, 1.40. Found: C, 26.33; H, 0.48; N, 1.19%. IR (ν CO) in CH_2Cl_2: 2064 s, 2055 s, 2025 s, 2013 s, br, 1994 br, 1979 w, br cm^{-1}. ^{1}H-NMR of **7** at 400 MHz in $CDCl_3$: δ 9.79 (s, H(2)), 9.24 (d, H(9)), 8.68 (d, H(7)), 8.48 (d, H(3)), 7.97 (dd, 2H(4 and 6)), 7.76 (dd, H(5)), 7.31 (dd, H(8)), −12.11 (s, hydride).

Compound **8**: Anal. Calc. for $C_{22}H_9NO_9Os_3$: C, 26.37; H, 0.90; N, 1.40. Found: C, 26.55; H, 1.21; N, 1.51%. IR (ν CO) in CH_2Cl_2: 2074 m, 2045 s, 2020 s, 1989 m, br, 1971 w cm^{-1}. ^{1}H-NMR of **8** at 400 MHz in $CDCl_3$: δ 9.03 (dd, H(2)), 8.68 (dd, H(4)), 8.32 (d, H(8)), 7.98 (d, H(5)), 7.89 (dd, H(6)), 7.71 (dd, H(7)), 7.55 (s, H(9)), 7.18 (dd, H(3)), −12.41 (s, hydride).

Compound **9**: Anal. Calc. for $C_{17}H_8N_2O_9Os_3$: C, 21.38; H, 0.84; N, 2.94. Found: C, 21.45; H, 0.67; N, 2.86%. IR (ν CO) in CH_2Cl_2: 2073 m, 2043 s, 2014 s, 1984 br, 1942 w, br cm^{-1}. ^{1}H-NMR of **9** at 400 MHz in $CDCl_3$: δ 8.72 (s, br, NH), 8.16 (dd, 2H(4 and 6)), 6.98 (dd, H(5)), 2.74 (s, CH_3), −11.78 (s, hydride).

Compound **10**: Anal. Calc. for $C_{16}H_7N_3O_9Os_3$: C, 20.10; H, 0.73; N, 4.40. Found: C, 20.15, H, 0.42; N, 4.29%. IR (ν CO) in CH_2Cl_2: 2080 m, 2052 s, 2021 s, 1993 s, br, 1956 w, br, 1941 w, br cm^{-1}. ^{1}H-NMR of **10** at 400 MHz in $CDCl_3$: δ 8.58 (d, H(6)), 8.46 (d, H(4)), 7.24 (dd, H(5)), 4.46 (s, CH_3), −11.91 (s, hydride).

Compound **11**: Anal. Calc. for $C_{17}H_7NO_{10}Os_3$: C, 21.36; H, 0.73; N, 1.47. Found: C, 21.47; H, 0.54; N, 1.43%. IR (ν CO) in CH_2Cl_2: 2078 s, 2049 s, 2021 s, 1990 s, br, 1952 w, 1942 w, br cm^{-1}. ^{1}H-NMR of **11** at 400 MHz in $CDCl_3$: δ 8.28 (dd, 2H(4 and 6)), 7.09 (dd, H(5)), 2.91 (s, CH_3), −11.91 (s, hydride).

Compound **12**: Anal. Calc. for $C_{16}H_5NO_9SOs_3$: C, 20.06; H, 0.52; N, 1.46. Found: C, 20.15; H, 0.38; N, 1.36%. IR (ν CO) in CH_2Cl_2: 2072 s, 2050 s, 2022 s, 1992 s, br, 1954 w, 1941 w, br cm^{-1}. ^{1}H-NMR of **12** at 400 MHz in $CDCl_3$: δ 9.04 (s, H(2)), 8.74 (dd, H(6)), 8.58 (dd, H(4)), 7.18 (dd, H(5)), −11.84 (s, hydride).

Compound **13**: Anal. Calc. for $C_{17}H_7NO_9Os_3$: C, 21.01; H, 0.72; N, 1.44. Found: C, 21.22; H, 0.61; N, 1.34%. IR (ν CO) in CH_2Cl_2: 2076 m, 2049 s, 2019 s, 1989 s, br, 1952 w, br cm^{-1}. ^{1}H-NMR of **13** at 400 MHz in $CDCl_3$: δ 8.59 (dd, H(6)), 8.44 (dd, H(4), 7.09 (dd, H(5)), 3.03 (s, CH_3), −12.03 (s, hydride).

Compound **14**: Anal. Calc. for $C_{17}H_6N_2O_9Os_3$: C, 21.43; H, 0.63; N, 2.94. Found: C, 21.46; H, 0.48; N, 2.83%. IR (ν CO) in CH_2Cl_2: 2077 s, 2051 s, 2020 s, 1991 br, 1952 w, 1941 w, br cm^{-1}. ^{1}H-NMR of **14** at 400 MHz in $CDCl_3$: δ 9.15 (d, H(2)), 8.72 (dd, H(7)), 8.67 (dd, H(5)), 8.54 (d, H(3)), 7.46 (dd, H(6)), −12.16 (s, hydride).

*4.2. Preparation of $[Os_3(CO)_9(\mu_3\text{-}\eta^3\text{-}C_9H_6(R)(R')N)(\mu\text{-}H)]$ (**3b**, R = 3-CO_2CH_3, R′ = 5-$C(CH_3)_2CN$; **3d**, R = 4-CH_3, R′ = 5-$C(CH_3)_2CN$; **3g**, R = 4-NH_2, R′ = 5-$C(CH_3)_2CN$; **3h**, R = 4-CO_2CH_3, R′ = 5-$CH_2CH{=}CH_2$; cis-**3p**, R = 6-CO_2CH_3, R′ = 5-$CH_2CH{=}CH_2$; **6′**, R = 5-NH_2, R′ = 4-$C(CH_3)_2CN$)*

The following procedure was followed for the compounds listed above. A 25–200 mg (0.025–0.20 mmol) sample of $[Os_3(CO)_9(\mu_3\text{-}\eta^2\text{-}C_9H_5(R)N)(\mu\text{-}H)]$ was dissolved in 5 ml THF and cooled to −78°C, at which time a 1.5–3 molar excess of the appropriate carbanion was added slowly by syringe. The amount of carbanion added was governed by an observable color change from deep green to dark amber or orange. The reaction mixture was warmed to 0°C, stirred for 0.25–1 h, cooled again to −78°C and quenched with an amount of trifluoroacetic acid, 10% in excess of the amount of carbanion used. The solution generally turned orange–red as it warmed to r.t. The clear orange–red solution then rotary evaporated, taken up in minimum CH_2Cl_2, filtered and then purified by thin layer chromatography on $0.1 \times 20 \times 20$ or $0.1 \times 20 \times 40$ cm silica gel plates using CH_2Cl_2/hexanes (20–50% CH_2Cl_2 as eluent. In general, one major orange band containing the nucleophilic addition product was observed in addition to minor amounts of unconsumed starting material. Yields are given along with the analytical and spectroscopic data below.

Compound **3d**: yield for **3d**: 71.2%. Anal. Calc. for $C_{23}H_{16}N_2O_9Os_3$: C, 26.60; H, 1.54; N, 2.70. Found: C, 26.48; H, 1.49; N, 2.60%. IR (ν CO) in CH_2Cl_2: 2080 s, 2050 s, 2026 s, 1990 br, 1968 w, 1954 w cm^{-1}. ^{1}H-NMR of **3d** at 400 MHz in $CDCl_3$: δ 8.42 (dd, H(2)), 6.77 (d, H(3)), 3.92 (m, H(7)), 2.97 (dd, H(5)), 2.73 and 2.09 (m and m, H(6) 2 protons), 2.19 (s, CH_3 on C(4)), 1.46 and 1.42 (s and s, CH_3 6 protons), − 17.022 (s, hydride).

Compound **3b**: yield for **3b**: 50.3%. Anal. Calc. for $C_{24}H_{17}N_2O_{11}Os_3$: C, 26.64; H, 1.57; N, 2.59. Found: C, 26.48; H, 1.34; N, 2.57%. IR (ν CO) in CH_2Cl_2: 2082 s, 2051 s, 2028 s, 1994 br, 1971 w cm^{-1}. ^{1}H-NMR of **3b** at 400 MHz in $CDCl_3$: δ 9.13 (s, H(2)), 8.02 (s, H(4)), 3.49 (s, CH_3 on carboxy), 3.87 (m, H(7)), 2.65 (d, H(5)), 2.83 and 2.22 (dd and q of q, H(6) 2 protons), 1.39 and 1.37 (s and s, CH_3 6 protons), − 17.03 (s, hydride).

Compound **3h**: yield for **3h**: 50.2%. Anal. Calc. for $C_{23}H_{15}N_1O_{11}Os_3$: C, 26.24; H, 1.42; N, 1.33. Found: C, 26.49; H, 1.52; N, 1.48%. IR (ν CO) in CH_2Cl_2: 2080 s, 2050 s, 2026 s, 1990 br, 1968 w, 1954 w cm^{-1}. ^{1}H-NMR of **3h** at 400 MHz in $CDCl_3$: δ 8.53 (d, H(2)), 7.29 (d, H(3)), 5.71 (m, allyl proton), 5.05 and 4.97 (dd and dd, terminal 2 allyl protons), 3.92 (m, H(7)), 3.89 (s, CH_3 on carboxy), 3.55 (dd, H(5)), 2.51 and 2.31 (m and m, H(6) 2 protons), 1.92 (qq, 1st allyl 2 protons), − 17.01 (s, hydride).

Compound *cis*-**3p**: yield for *cis*-**3p**: 57.2%. Anal. Calc. for $C_{23}H_{15}N_1O_9Os_3$: C, 26.24; H, 1.43; N, 1.33. Found: C, 26.16; H, 1.35; N, 1.30%. IR (ν CO) in CH_2Cl_2: 2080 s, 2050 s, 2026 s, 1990 br, 1968 w, 1954 w cm^{-1}. ^{1}H-NMR of *cis*-**3p** at 400 MHz in $CDCl_3$: δ 8.43 (d, H(2)), 7.30 (d, H(4)), 6.81 (t, H(3)), 5.61 (m, 2nd H on allyl), 4.97 and 4.78 (m and m, terminal allyl 2 protons), 4.15 (d, H(7)), 3.82 (s, CH_3 on carboxy), 3.09 (m, 1st allyl proton), 2.99 (m, H(6)), 2.27–2.23 (m, H(5) and 1st proton of allyl), − 17.09 (s, hydride).

Compound **6′**: Yield for **6′**: 51.2%. Anal. Calc. for $C_{22}H_{15}N_3O_9Os_3$: C, 25.51; H, 1.54; N, 4.05. Found: C, 25.89; H, 1.69; N, 3.89%. IR (ν CO) in CH_2Cl_2: 2078 s, 2049 s, 2021 s, 1984 br, 1944 w cm^{-1}. ^{1}H-NMR of **6′** at 400 MHz in $CDCl_3$: δ 8.88 (dd, H(2)), 7.89 (d, H(6)), 6.27 (d, H(7)), 4.88 (s, NH_2), 3.20 (dd, H(4)), 3.15 and 3.01 (dd and d, H(3) 2 protons), 1.37 and 1.34 (s and s, CH_3 6 protons), − 13.78 (s, hydride).

*4.3. X-ray structure determination of **7–10**, **12** and **14***

Crystals of **7–10**, **12** and **14** for X-ray examination were obtained from saturated solutions of each in hexane/dichloromethane solvent systems at − 20°C. Suitable crystals of each were mounted on glass fibers, placed in a goniometer head on the Enraf–Nonius CAD4 diffractometer, and centered optically. Unit cell parameters and an orientation matrix for data collection were obtained by using the centering program in the CAD4 system. Details of the crystal data are given in Tables 4 and 5. For each crystal, the actual scan range was calculated by scan width = scan range + 0.35 tan θ and backgrounds were measured by using the moving-crystal moving-counter technique at the beginning and end of each scan. Two representative reflections were monitored every 2 h as a check on instrument and crystal

stability. Lorentz, polarization, and decay corrections were applied, as was an empirical absorption correction based on a series of ψ-scans, for each crystal (except for **9** where no absorption correction was applied). The weighting scheme used during refinement was $1/\sigma^2$, based on counting statistics.

Each of the structures was solved by the Patterson method using SHELXS-86 [27], which revealed the positions of the metal atoms. All other non-hydrogen atoms were found by successive difference Fourier syntheses. The expected hydride positions in each were calculated by using the program HYDEX [28], hydrogen atoms were included in each structure and were placed in their expected chemical positions using the HFIX command in SHELXL-93 [29]. The hydrides were given fixed positions and U values; other hydrogen atoms were included as riding atoms in the final least-squares refinements with U values which were related to the atoms ridden upon. All other non-hydrogen atoms were refined anisotropically in **7**, **10**, and **12**; only the osmium and oxygen atoms were refined anisotropically for **9** and **14**; and only the osmium atoms in **8** could be refined anisotropically.

Scattering factors and anomalous dispersion coefficients were taken from the International Tables for X-ray Crystallography [30]. All data processing was carried out on a DEC 3000 AXP computer using the Open MolEN system of programs [31]. Structure solution, refinement and preparation of figures and tables for publication were carried out on PCs using SHELXS-86 [27], SHELXL-93 [29] and SHELXTL-PC [32] programs.

Acknowledgements

We gratefully acknowledge the support of the National Science Foundation (CHE 9625367) for support of this research. We also acknowledge helpful and stimulating discussions with Professor Charles Thompson. We also acknowledge the M.J. Murdock Trust for a summer fellowship (RH).

References

[1] L.A.P. Kane-Maguire, E.D. Honig, D.A. Sweigart, Chem. Rev. 84 (1994) 525.
[2] (a) L.A. Bromley, S.G. Davies, C.L. Goodfellow, Tet. Asymmetry 2 (1991) 139. (b) S.G. Davies, T.J. Donohoe, M.A. Lister, Tet. Asymmetry 2 (1991) 1089.
[3] M.F. Semmelhack, G.R. Clark, D.C. Garcia, J.J. Harrison, Y. Thebtarnonth, W.A. Wuff, A. Yamashita, Tetrahedron 37 (1981) 3957.
[4] S. Shouheng, L.K. Yeung, D.A. Sweigart, T.Y. Lee, S.S. Lee, Y.K. Chung, S.R. Switzer, R.D. Pike, Organometallics 14 (1995) 2613.
[5] U.S. Gill, R.M. Moriarty, Y.Y. Ku, I.R. Butler, J. Organomet. Chem. 417 (1991) 313.
[6] R.H. Fish, E. Baralt, H.S. Kim, Organometallics 10 (1991) 1965.
[7] J.A. Gladysz, G.A. Stark, A.M. Arif, Organometallics 13 (1994) 4523.
[8] S.E. Kabir, D.S. Kolwaite, E. Rosenberg, K. Hardcastle, W. Cresswell, J. Grindstaff, Organometallics 14 (1995) 3611.
[9] E. Arcia, D.S. Kolwaite, E. Rosenberg, K.I. Hardcastle, J. Ciurash, R. Duque, L. Milone, R. Gobetto, D. Osella, M. Botta, W. Dastru', A. Viale, J. Fiedler, Organometallics 17 (1998) 415.

[10] A. Bar Din, B. Bergman, E. Rosenberg, R. Smith, W. Dastru', A. Viale, L. Milone, R. Gobetto, Polyhedron 17 (1998) 2975.
[11] B. Bergman, R. Holmquist, R. Smith, E. Rosenberg, J. Ciurash, K.I. Hardcastle, M. Visi, J. Am. Chem. Soc. 120 (1998) 12818.
[12] G. Jones, in: G. Jones (Ed.), Quinolines, Wiley-Interscience, London, 1977.
[13] (a) J.M. Schaus, E.C. Kornfeld, R.D. Titus, C.L. Nichols, D.L. Huser, J.A. Clemens, E.B. Smatstig, R.W. Fuller, Drug Des. Disc. 9 (1993) 323. (b) I. Van Wijngaarden, M. Tulp, Eur. J. Pharmacol. 188 (1990) 301.
[14] (a) J.P. Michael, Nat. Prod. Rep. 12 (1995) 77. (b) M. Alvarez, M. Salas, J.A. Joule, Heterocycles 32 (1991) 759.
[15] M.F. Semmelhack, in: F.G.A. Stone, E. Abel, G. Wilkinson (Eds.), Comprehensive Organometallic Chemistry II, vol. 12, Elsevier-Interscience, Oxford, 1995, p. 979.
[16] G. Lavigne, in: D.F. Shriver, H.D. Kaesz, R.D. Adams (Eds.), The Chemistry of Metal Cluster Compounds, VCH, New York, 1990, Ch. 5.
[17] F.A. Bovey, NMR Data Tables for Organic Chemists, Wiley Interscience, New York, 1967.
[18] S. Aime, M. Botta, R. Gobetto, D. Osella, F. Padovan, J. Organomet. Chem. 353 (1988) 251.
[19] J.R. Shapley, D.E. Samkoff, C. Bueno, M.R. Churchill, Inorg. Chem. 21 (1982) 634.
[20] K.A. Azam, M.B. Hursthouse, S.A. Hussain, S.E. Kabir, K.M.A. Malik, M.M. Rahman, E. Rosenberg, J. Organomet. Chem. 559 (1998) 81.
[21] K.I. Hardcastle, E. Rosenberg, R. Smith, Organometallics (1999) in press.
[22] J.P. Coleman, L.S. Hegedus, J.R. Norton, R.G. Fink, Principles and Applications of Organotransition Metal Chemistry, University Science Books, Mill Valley, CA, 1987, p. 96.
[23] M.F. Semmelhack, W. Sanfert, K. Keller, J. Am. Chem. Soc. 102 (1980) 6584.
[24] J. Lewis, P.J. Dyson, B.J. Alexander, B.F.G. Johnson, C.M. Martin, J.G.M. Nairn, E. Parsini, J. Chem. Soc. Dalton Trans. (1993) 981.
[25] L. Bradford, T.J. Elliot, F.M. Rowe, J. Chem. Soc. (1947) 437.
[26] M. Hauser, J. Org. Chem. 15 (1950) 4612.
[27] G.M. Sheldrick, Acta Crystallogr. A46 (1990) 467.
[28] A.G. Orpen, J. Chem. Soc. Dalton Trans. (1980) 2509.
[29] G.M. Sheldrick, Program for Structure Refinement, University of Göttingen, Germany, 1993.
[30] A.J.C Wilson (Ed.) International Tables for X-ray Crystallography, vol. C, Kluwer, Dordrecht, 1992, Tables 6.1.1.4, pp. 500–502 and 4.2.6.8, pp. 219–222.
[31] C. Fair Kay, MOLEN Structure Determination System, Enraf–Nonius, Delft, The Netherlands, 1990.
[32] SHELXTL-PC, Siemens Analytical X-ray Instruments, Inc., Madison, WI, USA, 1993.